Fire Safety Journal 163 (2026) 104794

Contents lists available at ScienceDirect

Fire Safety Journal

journal homepage: www.elsevier.com/locate/firesaf

Dynamic fire emission of smoldering peat under water suppression

Yuting Jiang [a,b], Haoyang Qin [a,c], Chuan Wan [a], Yichao Zhang [b], Shaorun Lin [b], Jiuling Yang [c], Yuqi Hu [a,*], Xinyan Huang [b,**]

[a] Sichuan Fire Science and Technology Research Institute of MEM, Chengdu, China
[b] Research Centre for Fire Safety Engineering, Department of Building Environment and Energy Engineering, The Hong Kong Polytechnic University, Hong Kong
[c] School of Engineering, Sichuan Normal University, Chengdu, China

ARTICLE INFO

Keywords:
Gas emission
Fire suppression
Smoldering combustion
Emission factor
Water spray

ABSTRACT

The persistent smoldering peat fires are most difficult to extinguish because of their hidden nature and resurgence from underground. This study experimentally investigated the effects of water spray (fixed at 0.4 L/min or 600 mm/h) on the smoldering peat sample (20 cm × 20 cm × 10 cm) and associated gas emissions. The spray duration varied from 10 to 150 s, equivalent to water depths up to 25 mm. The dynamic emissions of CH_4, CO, CO_2, NH_3, and C_6H_{14} were measured during the burning and suppression. After water spray, three distinct outcomes were observed: failed, partial, or complete fire suppression. Notably, an accumulated water depth below 25 mm failed to achieve complete fire suppression. In cases of failed suppression, the smoldering fire resurged and ultimately consumed all peat. With increasing water volume, both the time to resurgence and the subsequent emission peak were delayed. The peak mass fluxes and emission factors (EF) of CO_2 and CO, along with the modified combustion efficiency (MCE) and CO/CO_2 ratio, exhibited weak dependence on water volume. In contrast, at the threshold water depth of 25 mm, the peak mass flux and EF of CH_4, as well as the CH_4/CO_2 ratio, decreased by approximately 50%. This work advances the scientific understanding of transient gaseous emissions from hidden underground peat fires subjected to water suppression.

1. Introduction

Global climate change has significantly increased the frequency and intensity of wildfires, making them as one of the most severe ecological disasters and public emergencies worldwide [1]. Smoldering combustion is a slow, flameless, and low-temperature form of burning. It often occurs and spreads in subsurface layers of duff and peat, with temperatures between 300 and 600 °C [2]. Smoldering fires can persist underground in peatlands for days or even months, making them among the most widespread and long-lasting wildfire phenomena. Due to their hidden nature and potential to transition into more destructive flaming wildfires, smoldering fires present a serious threat [2]. Such a transition leads to a sharp rise in fire temperature, heat release rate, and spread speed, resulting in considerably greater damage [3]. Therefore, a systematic study on smoldering fire suppression is critically needed.

As a typical form of incomplete combustion, smoldering emits more carbon monoxide (CO), methane (CH_4), ammonia (NH_3), and particulate matter (PM) than flaming combustion, while carbon dioxide (CO_2) is relatively lower [4–6]. A smoldering front comprises four distinct sub-fronts: preheating, evaporation, pyrolysis, and oxidation [7,8]. The pyrolysis front (above 200 °C in the absence of oxygen) generates char and releases volatile organic compounds, along with small amounts of CO_2, CO, and water vapor. In the char oxidation front (typically above 350 °C), large quantities of CO_2 and CO are produced. Hu et al. [9] showed that smoldering emissions evolve with different gas species dominating during various combustion stages (ignition, growth, steady and burn out). Emissions of alkanes, such as CH_4, which has about 28-35 times higher global warming potential than CO_2, peak during the ignition stage. In contrast, CO_2, CO, and NH_3 increase during the steady stage [9]. Yang et al. [10] found in thermogravimetric analysis (TGA) of peat pyrolysis, CH_4 emissions increased with heating rate, while CO_2 and CO were not sensitive to heating rate. Similar findings were observed in meso-scale peat fire experiments [11]. In these tests, CH_4 emissions dropped rapidly as peat moisture increased,

This article is part of a special issue entitled: FISJ_IAFSS 2026 published in Fire Safety Journal.

* Corresponding author.
** Corresponding author.
E-mail addresses: huyuqi@scfri.cn (Y. Hu), xy.huang@polyu.edu.hk (X. Huang).

https://doi.org/10.1016/j.firesaf.2026.104794
Received 25 September 2025; Received in revised form 13 March 2026; Accepted 26 March 2026
Available online 27 March 2026

but they increased with higher oxygen supply [11].

In the literature, the roles of fuel physicochemical properties (such as moisture content, bulk density, and elemental composition) influencing the fire emissions have been widely investigated. Garg et al. [12] studied the effects of fuel moisture content on emissions, and found that its influence varies across fuel types, with chemical composition being a more critical factor. Similarly, Hu et al. [13] found that heterogeneous physicochemical properties of peatlands, especially moisture content, significantly affect the emission factors of major gas species, including CO_2, CO, and CH_4. Other studies have investigated how fuel bed heterogeneity, specifically particle size distribution, impacts smoldering behavior and emissions [14–16]. The results indicate that variations in particle size affect oxygen supply and heat transfer, thereby altering smoldering spread and gas emissions. Furthermore, Deane et al. [17] showed that physical properties like ground cover and compression are key determinants of smoldering emissions, with compressed moss and peat plots exhibiting significantly lower fire danger. Beyond fuel properties, airflow and oxygen supply are critical environmental factors. Wang et al. [18] reported that as oxygen concentration increases, the emission factors of CO_2 and CO also rise. They also observed higher emissions of hydrocarbons, especially CH_4, due to enhanced oxygen availability.

Current techniques for suppressing smoldering fires rely mainly on cooling, with water-based methods being the most effective and widely used [19]. Natural precipitation (i.e., rainfall and snowfall) can suppress smoldering wildfires on a scale beyond human firefighting capabilities. Vasconcelos et al. [20] have shown that increased rainfall significantly reduces burned areas in wildland fires. However, if smoldering is not completely extinguished by rain, it can reignite after a long period, especially during dry or windy seasons [21]. Unlike flaming fires, the success of suppressing hidden smoldering fires cannot be immediately confirmed by visual inspection [22].

Recent laboratory-scale studies have investigated various cooling methods for suppressing smoldering fires, including sprinkler spray simulating rainfall [22], water injection via nozzles [23,24], water spray [25,26], buried cooling pipes [27], snowfall and ice [28,29], dry ice, liquid nitrogen [30], and water-filled trenches [31]. Among these methods, nozzle injection and buried pipes are less efficient than water spray, requiring a greater water volume under similar fire conditions. Water-filled trenches can be ineffective in areas with low groundwater levels and are labor-intensive as they require deep excavation [31]. Consequently, liquid water spray is considered the most viable cooling method for suppressing smoldering fires. Lin et al. [19] determined a minimum rainfall intensity of 4 mm/h and a minimum rainfall depth of 13 mm for extinguishing the underground peat fire (15 cm deep) and highlighted the fire-suppression effectiveness of short-term heavy rainfall. Ramadhan et al. [25] found that a continuous water spray of 12 L/h for 65 min (or 1300 mm equivalent water depth) was required to extinguish a 10 cm deep peat smoldering fire. Santoso et al. [26] reported that the total water volume required to suppress peat smoldering is constant at 5.7 ± 2.1 L/kg of peat (or 57 mm equivalent water depth), emphasising the physical role of water in suppression over its chemical role. Thus, the threshold water depth for suppressing peat fire varies from 13 mm to 1300 mm, showing a large variety in experimental design (e.g., water droplet size, timing and uniformity of water suppression) as well as the complex and persistent nature of peat fires [22,25,26].

While considerable research has focused on suppressing smoldering combustion, the associated gas-emission hazards during water-based suppression remain poorly understood. Current global fire emission inventories (e.g., GFED [32]) fail to adequately account for the impact of precipitation, limiting the accurate estimation of carbon budgets from fire events. In addition, quantifying transient emissions during smoldering fire suppression is crucial for evaluating the occupational exposure and health risks of firefighters.

This study investigates the impact of water spray on smoldering suppression and its associated dynamic gas emissions under different fire development stages. Findings from this study address this research gap and provide insights for improving smoldering extinguishing strategies with effective gas emission control.

2. Materials and methods

The sample used in this study was a commercially available Danish peat (Pindstrup Co., Denmark). The element analysis (Elemantar-Vario EL cube) presents mass fractions of 45.09 ± 1.30%, 6.16 ± 0.27%, 46.76 ± 1.16%, and 1.29 ± 0.19% for C, H, O, and N, respectively. Before the experiments, the peat samples were oven-dried at a constant temperature of 90 °C for 18 h [9,33]. The dried peat samples were then crushed and sieved to obtain particles within a size range of 0.425 mm ≤ d < 4 mm, after which they were mixed evenly. The measured moisture content on a dry basis (the mass of water divided by the mass of dry sample) and the bulk density of the prepared peat samples were 25 ± 5% and 177 ± 3 kg/m^3, respectively.

As shown in Fig. 1(a), an experimental platform for smoldering fire suppression was designed and built to obtain mass loss (DJ 10K-2 balance), real-time gas emissions (SSCM-V2 Fourier-transform infrared spectroscopy (FTIR)), temperature distribution (24 K-type thermocouples), surface visual (GoPro Hero 10), and infrared (IR) imaging (HIKMICRO 256 infrared camera) of the peat bed [14,34]. The thermocouples (1 mm diameter) were arranged in a matrix of 4 (vertical) × 6 (horizontal) within the reactor, as shown in Fig. 1(b). Data from the balance, thermocouples, and visual and IR images were logged at a frequency of 1 Hz. The FTIR monitored real-time concentrations of 5 gas species at a data acquisition frequency of 0.2 Hz: carbon dioxide (CO_2), carbon monoxide (CO), methane (CH_4), ammonia (NH_3), and hexane (C_6H_{14}).

A stainless-steel open-top reactor, with internal dimensions of 20 cm × 20 cm × 10 cm and a wall thickness of 2 cm, was used to burn the samples. Five circular drainage holes with a diameter of 2 cm were distributed at the bottom of the reactor to simulate natural water infiltration in peat layers. A cylindrical igniter was installed at the midpoint of the left side of the reactor. Following the ignition protocol described in Ref. [33], we applied 100 W for 30 min to initiate a uniform smoldering spread.

An automated water spray system was designed for smoldering fire suppression. The water spray system was activated at t = 300 min. This activation time was selected because preliminary experiments showed that under natural smoldering conditions without suppression intervention, the mass loss rate (MLR, g/s) of the sample reached its peak at approximately 300 min after ignition, indicating a fully developed, self-sustained smoldering spread. The spray nozzle was positioned at the location of the smoldering front. The spray flow rate was fixed at 0.4 L/min, corresponding to a rainfall intensity of 600 mm/h. According to the literature on rain suppression [19], this intensity fell within the category of violent rain. The spray durations (Δt_s, s) of 10 s, 30 s, 60 s, 120 s, and 150 s were controlled by an electronic start-stop valve. These spray durations corresponded to water volumes per unit mass of peat ranging from 0.094 L/kg to 1.41 L/kg, or to an equivalent water depth up to 25 mm for a fuel bed with a cross-section of 20 cm × 20 cm, as summarized in Table 1. System calibration confirmed that, with the flow rate set at 0.4 L/min, the discrepancy between theoretical and actual water volumes was within 2.8% − 3.0%.

Throughout the experiments, the combustion chamber was maintained at a stable temperature of 20 °C and a relative humidity of 40%, which helped minimize environmental effects on the data. To ensure reproducibility, each condition was repeated at least three times.

3. Results and discussion

3.1. Outcomes of water spray suppression

When the water spray (600 mm/h) duration is below 150 s (or 2.5

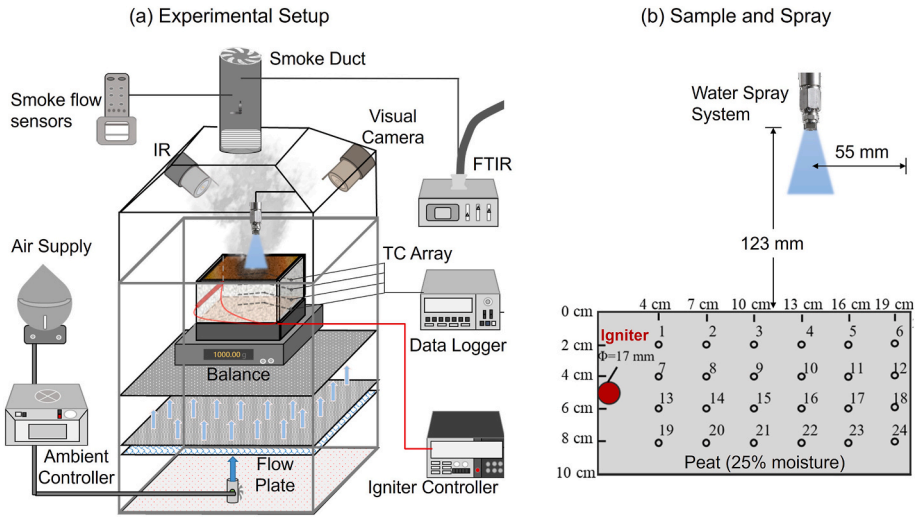

Fig. 1. (a) Schematic of the experimental platform for smoldering fire suppression and (b) the thermocouples array.

Table 1
Water spray characteristics under a fixed spray intensity of 600 mm/h.

Spray Duration (s)	10	30	60	120	150
Spray Duration (min)	1/6	1/2	1	2	2.5
Water volume (L)	0.07	0.2	0.4	0.8	1.0
Water-to-peat ratio (L/kg)	0.094	0.28	0.56	1.23	1.41
Equivalent water depth (mm)	1.7	5	10	20	25

min), corresponding to an equivalent water depth of below 25 mm, the smoldering fire can not be suppressed, and the peat is completely burnt out in the reactor. When the sprayed water depth is increased to 25 mm, three fire-suppression outcomes are observed and categorized as: (a) failed suppression; (b) partial suppression; and (c) complete suppression (extinguishment), showing the water-suppression threshold in Fig. 2 and Video S1. It is worth noting that this threshold value of 25 mm lies between the 13 mm [19] and 57 mm [26] thresholds reported in the literature, despite differences in experimental design and the complexity of peat fires.

This fire-suppression process depends on a balance between two key factors: sufficient residual heat to initiate pyrolysis at the unburned peat (heat transfer) and adequate oxygen transport to sustain char oxidation (oxygen supply) [35]. In this context, water spray primarily alters the heat-transfer processes at the smoldering front, since fire spread is essentially a continuous ignition process. When suppression fails, the smoldering fire resurges and spreads throughout the entire sample, indicating that the water application could not disrupt the critical balance of heat and oxygen required for self-sustained smoldering. As the surrounding peat dries and oxygen availability increases, the smoldering front propagates into unburned fuel, ultimately establishing a new, self-sustaining front.

In partial suppression, the smoldering front reactivates only within the pre-existing char zone. Here, residual heat and oxygen are insufficient for it to propagate into adjacent, unburned peat. The fire thus consumes the limited fuel in the char zone until it self-extinguishes. Extinguishment is achieved when the applied water fully penetrates the peat bed, substantially cooling the fuel bed and saturating the pores, thereby blocking oxygen transport.

The varying outcomes for the same applied water volume highlight the stochastic nature of smoldering suppression. Subtle differences in peat properties (e.g., density, porosity, and initial moisture) significantly alter water penetration. As a result, despite a consistent spray setup, the actual water delivery to the smoldering front varied, ultimately dictating the suppression outcomes.

Smoldering temperatures typically range from 300 to 600 °C [2]. Fig. 3 shows (a) the temperature evolution of a peat smoldering front and (b) the average duration of pyrolysis (>300 °C) during the resurgence stage, measured by the thermocouples under different water spray durations. Both the hibernation time and the time required to reach the maximum temperature (i.e., a sign of fire resurgence) post water

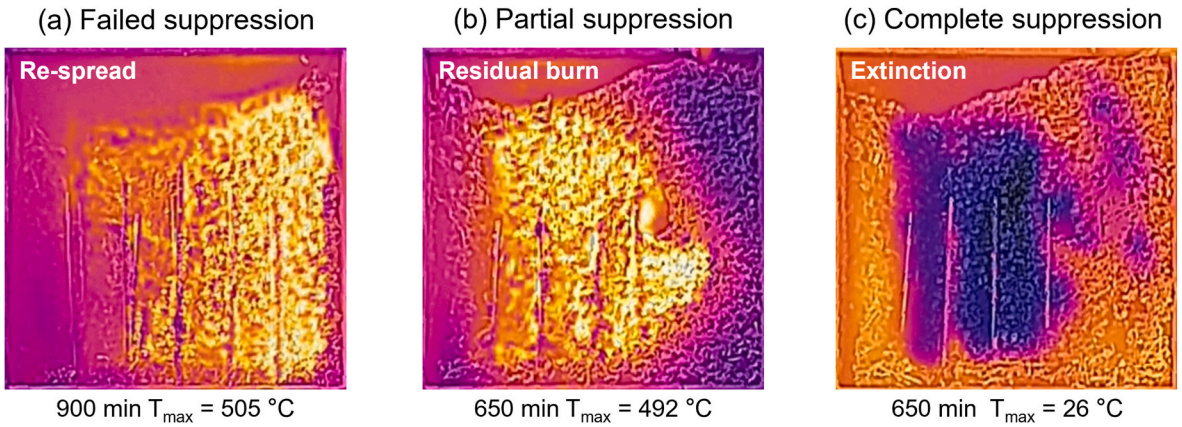

Fig. 2. IR imaging for three outcomes of peat fire under the same water-spray duration (150 s or 2.5 min): (a) failed suppression, (b) partial suppression, (c) complete suppression (extinguishment), where the water spray is equivalent to 25 mm water depth (see Video S1).

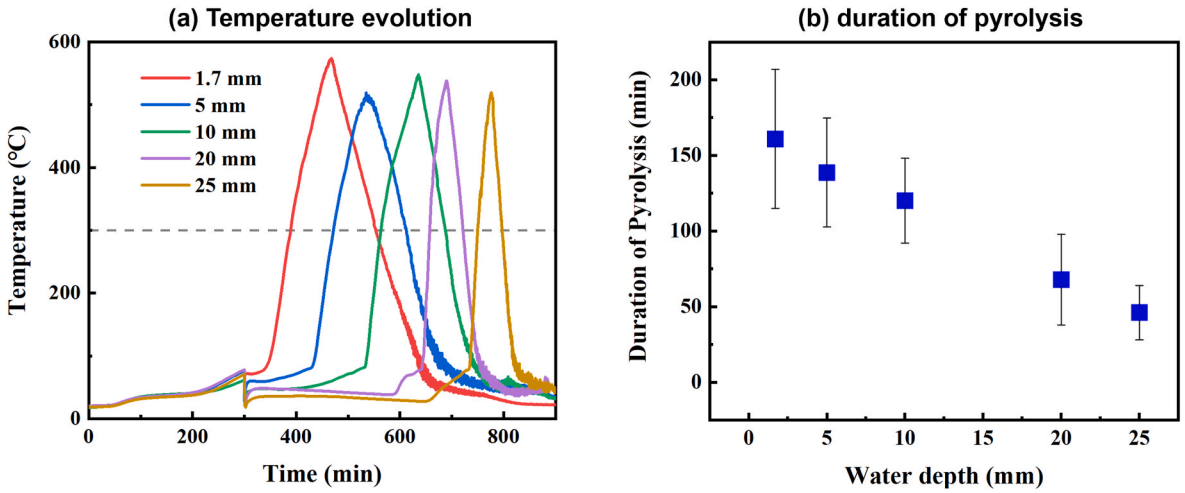

Fig. 3. (a) Temperature evolution at the peat smoldering front (Thermocouple #11) and (b) the average duration of pyrolysis (>300 °C) during the resurgence stage, after the water suppression and fire resurgence.

suppression increase with the duration and amount of water applied. Moreover, the average duration of pyrolysis decreases with increasing water volume, indicating reduced pyrolysis intensity.

3.2. Emission evolution under water suppression

Fig. 4 shows the gas-emission mass flux after water suppression for 2.5 min (equivalent to 25 mm water depth). Here, the gas mass flux $\left(\dot{m}''_{g,i}(t)\right)$ is defined as the mass flow rate per unit surface area [g/(s·m^2)] [6] for (a) CO_2, (b) CO, (c) CH_4, and (d) C_6H_{14} as

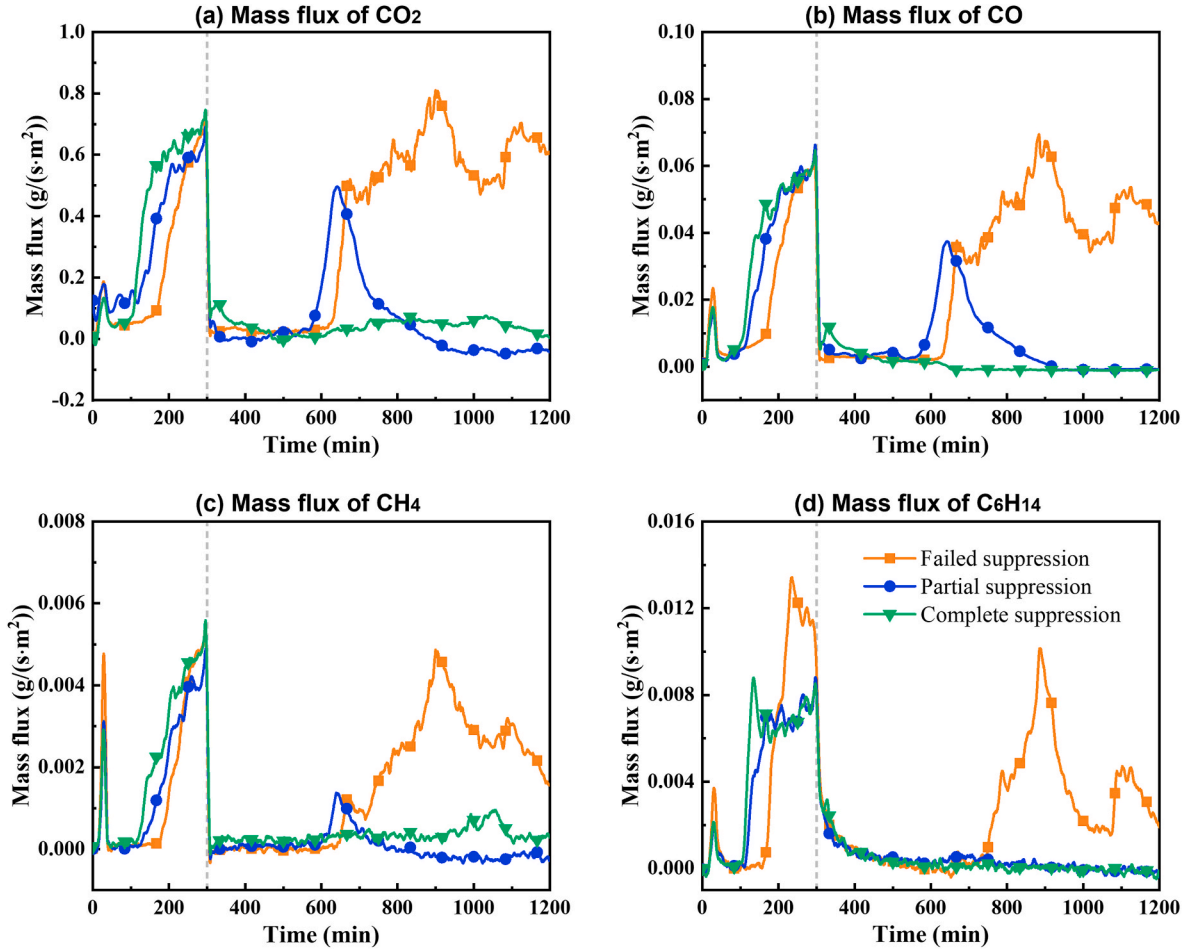

Fig. 4. Gas evolution of CO_2, CO, CH_4, and C_6H_{14} among the three distinct outcomes of smoldering peat fire after water suppression for 2.5 min (equivalent to 25 mm water depth).

$$\dot{m}''_{g,i}(t) = \frac{\rho_i \cdot [i](t) \cdot \dot{V}}{A} \quad (1)$$

where ρ_i is the density of gas species i (based on the ideal gas law under standard conditions, g/m^3); $[i](t)$ is the real-time concentration of species i (net concentration from the fire, ppm); $\dot{V}$ is the volumetric flow rate in the smoke duct (m^3/s); and A is the surface area of the sample (m^2).

The gas evolution curves show critical differences in the thermochemical reactions between local smoldering in the char zone and self-sustaining propagation into unburned peat. Upon water application at 300 min, a drastic decline in mass fluxes occurred, with levels reaching near-zero across all conditions. Following this quiescent period, the smoldering fire may resurge. Both partial and complete smoldering resurgence show an immediate, sharp increase in the mass flux of CO_2 and CO, reaching around 0.50 g/(s·m^2) and 0.037 g/(s·m^2), respectively. In contrast, hydrocarbon emissions remain notably low during this period, at approximately 0.0014 g/(s·m^2) for CH_4 and below 0.0001 g/(s·m^2) for C_6H_{14}. After water suppression, much of the heat generated from the pre-suppression smoldering front is retained. Upon drying of the peat and with sufficient oxygen supply, this retained heat primarily drives the heterogeneous oxidation of solid carbon within the char. This reaction can be represented [2,33] as

$$Char(s) + O_2 \rightarrow Heat + CO_2 + CO + H_2O + other\ gases + Ash(s) \quad (2)$$

These highly exothermic reactions produce CO_2 and CO as the main gaseous products. Because the smoldering front is confined to the already-pyrolyzed char, the release of complex volatile hydrocarbons from the peat is minimal. The partial suppression case, which exhibits only this stage, demonstrates that combustion fails to progress beyond this carbon oxidation phase, thus preventing the further pyrolysis of fresh peat [36].

In the failed suppression cases, the smoldering front propagates into unburned peat. This results in a sharp peak in hydrocarbon production, whereas CO_2 and CO mass fluxes show only a minor secondary rise. Quantitatively, the peak fluxes of CO_2 and CO (0.81 and 0.069 g/(s·m^2), respectively) are roughly double those observed during partial suppression (0.50 and 0.037 g/(s·m^2)). In contrast, the peak CH_4 flux (0.0048 g/(s·m^2)) is approximately three times higher than that of the partial suppression case (0.0014 g/(s·m^2)). This increase in hydrocarbon emissions indicates that, as smoldering proceeds, the width of the pyrolysis front increases and the pyrolysis reaction becomes significantly stronger [7].

Water application significantly alters the structure of the smoldering front, thereby altering the balance between pyrolysis and oxidation [19]. As the peat moisture content increases from water application, the thickness of the smoldering front decreases [7]. However, the oxidation front, being primarily controlled by oxygen diffusion, remains relatively unaffected. This leads to a narrower pyrolysis front [7], promoting near-immediate oxidation of volatiles within the active smoldering zone. However, as smoldering continues, the moisture content of the peat decreases ahead of the oxidation front, allowing the thermal front to expand. A wider thermal front increases the spatial and temporal window for fresh peat to undergo thermal decomposition prior to entering the high-temperature oxidation zone. Consequently, the thickness of the pyrolysis front also increases.

It is noteworthy that upon water spraying, CO_2, CO, and CH_4 exhibit an immediate and sharp decline to near-zero levels, indicating immediate quenching of the primary smoldering zone (Fig. 4). In sharp contrast, the mass flux of C_6H_{14} decreases at a significantly slower rate across all experimental conditions. Unlike the other gases, C_6H_{14} is a volatile organic compound with a relatively low boiling point (~69 °C). While the main pyrolysis and oxidation reactions are halted during water spraying, residual heat may still cause slow vaporization of liquid-phase hydrocarbons. This delayed vaporization allows C_6H_{14} to continue to be released after the active smoldering has ceased. Furthermore, the absence of detectable C_6H_{14} during partial suppression in Fig. 4 shows that it may have condensed in cooler regions of the peat bed or the smoke duct, preventing accurate measurement by the FTIR analyzer.

For the failed suppression cases, Fig. 5 illustrates the temporal evolution of a typical experiment during water suppression (spray duration: 2 min). A strong correlation is observed between the trends in mass loss rate and those of the major gaseous emission fluxes. According to Ref. [9], the natural smoldering combustion of peat without water suppression can be divided into four stages: ignition, growth, steady, and burnout. Under water suppression conditions, four distinct evolution stages are observed: (I) the initial development stage (before water spray, 0 − 300 min), (II) the apparent quenching stage (characterized by a decline in MLR following water spray and subsequent stabilization), (III) the smoldering resurgence stage (marked by a renewed increase in MLR), and (IV) the burnout stage (when the smoldering front reaches the right wall of the reactor and the fuel is completely consumed).

During the initial development stage, the evolution is consistent with that observed in smoldering conditions without suppression [9]. The external heating source from the ignitor provides substantial thermal energy, inducing the pyrolysis of peat, which leads to the formation of char and the release of pyrolysis gases [7]. At t = 30 min, the MLR reaches its first peak at 0.019 g/s. The mass fluxes of CO_2, CO, and CH_4 simultaneously reach their respective first peak values at 0.16 g/(s·m^2), 0.030 g/(s·m^2), and 0.0098 g/(s·m^2), respectively. In contrast, NH_3 emissions are not detected during this period. This absence can be attributed to the water-retaining capacity of the peat's porous structure, which enables physical adsorption or dissolution of hydrophilic polar gases, thus preventing the release of NH_3 into the gas phase [11]. After the igniter is turned off, both the MLR and gaseous mass flux decrease sharply. Subsequently, the heat generated by char oxidation leads to self-sustaining smoldering. As a result, the MLR and mass fluxes of CO_2, CO, CH_4, and NH_3 gradually increase. At t = 300 min, the smoldering process has reached a steady state, and the water spray is triggered.

Following the water spray intervention, the peat fire enters the apparent quenching stage, with gas emissions dropping to near-zero levels. Infrared imaging reveals an immediate and rapid drop in the peak surface temperature of the peat sample during water spray. The intense forced cooling rapidly inhibits both pyrolysis and oxidation reactions [37], resulting in a sharp decline in the mass flux of gaseous emissions. The abrupt introduction of water also leads to significant fluctuations in MLR. Subsequently, the MLR gradually decreases, reflecting a progressively slowing water evaporation rate. The evaporation process extracts substantial heat, causing a drop in the overall temperature of the peat surface. The sample thus reaches a prolonged thermally quenched state, with its surface temperatures stabilizing below 60 °C. During this period, the MLR remains below 0.005 g/s, and gas emissions are nearly negligible. This apparent quiescence at the surface poses a significant risk, as it may lead firefighters to prematurely conclude that the fire is extinguished, while smoldering may persist beneath the surface.

Around t = 550 min, both MLR and mass fluxes of gas emissions begin to rise again. Infrared imaging reveals the resurgence of localized smoldering within the pre-charred region. As it propagates through this region, the accumulated heat ultimately becomes sufficient to initiate pyrolysis in the adjacent, unburned peat ahead of the original smoldering front [7]. A new self-sustaining smoldering front then forms and propagates laterally toward the right side of the reactor. As the smoldering area expands, the MLR and mass fluxes of gas emissions rise rapidly, reaching a renewed steady state at around t = 640 min. When the smoldering front eventually reaches the right wall of the reactor, both MLR and the gas emissions peak again.

During the burnout stage, the smoldering process becomes influenced by the boundary effects [9]. The overall surface temperature of the sample drops below 400 °C. The surface gradually subsides due to

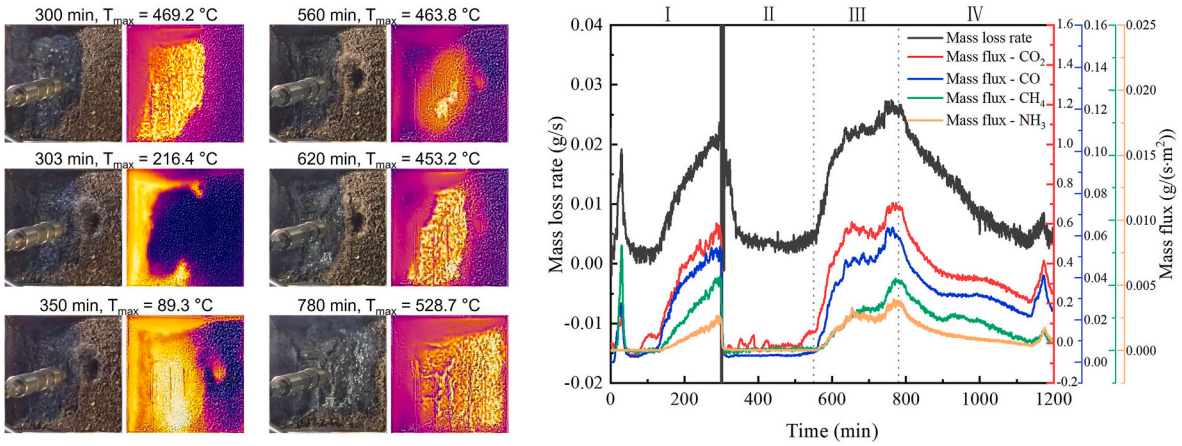

Fig. 5. Example evolution of visual and thermal imaging (left), and mass loss rate of peat sample, mass fluxes of CO_2, CO, CH_4 and NH_3 (right), after water suppression of a peat fire for 2 min (equivalent to 20 mm water depth). The fire resurged after 200 min.

sustained mass loss as the reaction progresses, inducing a collapse and ignition of unburned peat adhering to the right wall of the reactor. A corresponding temperature rise is observed, rising from approximately 240 °C to above 500 °C, which coincides with minor peaks in both MLR and mass flux.

3.3. Effects of water volume on mass flux

Fig. 6 illustrates the impact of increasing water volume on the mass fluxes of CO_2, CO, CH_4, and NH_3. The peak mass fluxes of CO_2, CO, and NH_3 after resurgence show minimal dependence on water volume. This suggests that the production of these gases is primarily determined by the inherent properties of the peat and the presence of a persistent char oxidation front [14]. Once smoldering resumes, the fire consumes all available char and releases a fixed total amount of CO_2, CO, and NH_3.

Conversely, the peak mass flux of CH_4 decreases significantly from 0.0077 g/(s·m^2) to 0.0039 g/(s·m^2) when the water volume increases to 1.41 L/kg (150 s). This occurs because CH_4 is primarily generated within the pyrolysis front. A longer water application enables more effective heat extraction from deeper peat layers, thereby hindering the re-establishment of a stable, widespread pyrolysis front.

As the water volume increases, the apparent quenching stage is significantly prolonged. It shows the effectiveness of water in temporarily disrupting the smoldering front [21]. However, when the water

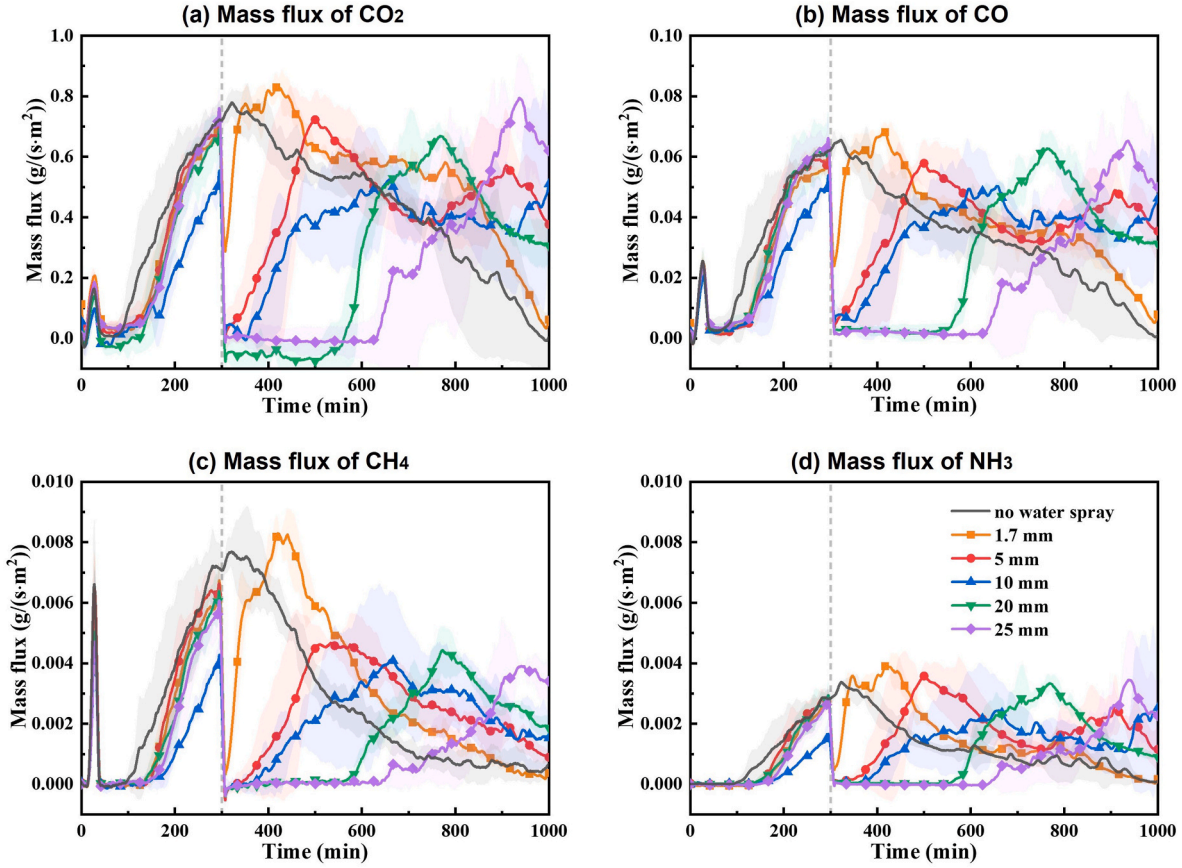

Fig. 6. Mass fluxes of CO_2, CO, CH_4, and NH_3 under different water volumes.

cooling is insufficient for complete suppression, the fire eventually resurges. Interestingly, for all failed suppression conditions, the characteristic times to resurgence and to emission peak, defined as the intervals from the start of the experiment ($t = 0$ min) to the first significant rise and to a local maximum of gas emissions in the post-suppression phase, respectively. This cooling period exhibits a positive correlation with the applied water volume, as demonstrated in Fig. 7. This finding offers firefighters a quantifiable metric for assessing suppression effectiveness. Such a metric can guide strategies for long-term monitoring, help allocate resources for re-inspection, and determine the critical window required to establish effective fire breaks before potential resurgence.

3.4. Effects of water volume on smoldering combustion

The emission factor is widely used to quantify total carbon emissions [18]. EF_m (g/kg) is defined as the mass of a specific emission per unit mass of dry fuel consumed [38] as:

$$EF_{m,i} = \frac{\dot{m}''_{g,i}(t)}{\left(\frac{\dot{m}_w(t)}{1+\varphi_w}\right)} \tag{3}$$

Where $\dot{m}''_{g,i}(t)$ is the instantaneous mass flux of emission i, g/(s·m^2); $\dot{m}_w(t)$ is the transient mass loss rate of the wet fuel measured by the balance, g/s; and φ_w is the initial moisture content of the fuel sample on a dry basis. However, accurately measuring the mass loss rate of fuel, especially in large-scale or field-based experiments, is often challenging. Therefore, many studies have utilized a carbon balance method to calculate the emission factor, EF_b (g/kg) [39–41]:

$$EF_{b,i} = F_c \cdot 1000\left(g\,kg^{-1}\right)\frac{MM_i}{12}\frac{C_i}{C_T} \tag{4}$$

where F_c is the measured carbon content of the dry fuel, %; MM_i is the molar mass of emission i, g/mol; C_i is the moles of emission i, mol; and C_T is the total moles of carbon released during combustion, mol.

Under the no-water-spray condition, the steady stage represents uninterrupted, free smoldering propagation [9], Fig. 8(a) presents the emission factors, both EF_m and EF_b, for CO_2, CO, and CH_4 during this steady stage under the no-water-spray condition. The good agreement between the EFs in two different forms indicates that the carbon emitted is proportional to the fuel consumed. Throughout the steady stage, the emission factors for CO_2 and CO remain relatively constant, whereas the EF for CH_4 exhibits a gradual increase.

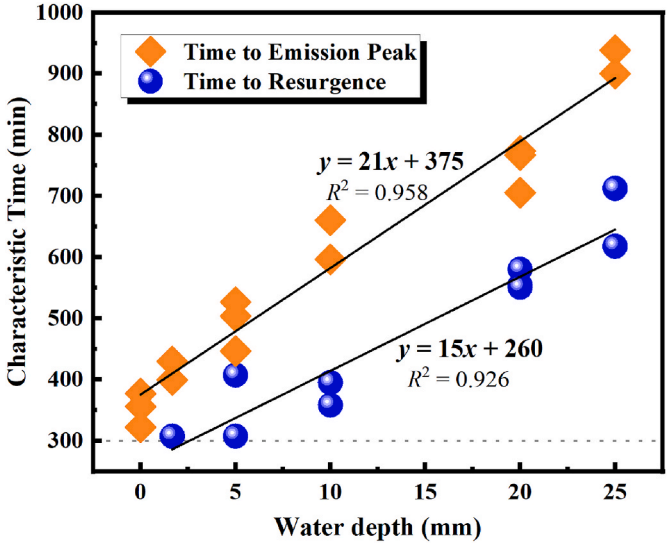

Fig. 7. Time to resurgence and to emission peak under varying water volumes.

The application of water interrupts the smoldering process. Fig. 8 (b–c) illustrates the transient EFs during stage II (apparent quenching) and stage III (smoldering resurgence) for the failed suppression and partial suppression cases, respectively. In the case of failed suppression, the fire re-establishes a renewed steady smoldering state after resurgence, with stable EFs matching those of the no-water-spray condition. In contrast, under partial suppression, smoldering is primarily confined to localized hotspots within the char zone and fails to re-stabilize, resulting in unstable EFs during smoldering resurgence.

The average EF_m and EF_b values for each renewed steady smoldering state under varying water volumes are shown in Fig. 9. The EF values for CO_2 and CO show little correlation with water volume. However, the EF values for CH_4 show a decreasing trend as water volume increases. This finding confirms that a larger water volume inhibits the re-establishment of an extensive pyrolysis front, and thus reduces hydrocarbon emissions.

The modified combustion efficiency (MCE) [39], the CO/CO_2 [7] and the CH_4/CO_2 [42] ratios are widely employed to characterize the smoldering emissions and the completeness of combustion. MCE is defined as MCE = $\Delta CO_2/(\Delta CO_2+\Delta CO)$, where Δ represents the excess mixing ratio (the difference between the species mole ratio in the smoke and that in ambient air). However, during the apparent quenching stage, gas emissions drop to extremely low levels, causing these ratios to fluctuate markedly. Consequently, they lack the precision required to characterize any smoldering that may continue within the fuel bed.

Fig. 10 presents the average values of these indicators during the renewed steady smoldering state. The MCE and the CO/CO_2 ratio show little correlation with water volume, with CO/CO_2 values (0.1– 0.2) consistent with literature reports for tropical peat [43,44]. By contrast, the CH_4/CO_2 ratio exhibits a clear decreasing trend as water volume increases.

4. Conclusions

This study investigated the impact of water spray (0.4 L/min) on peat smoldering suppression and the resulting transient gas emissions. For spray durations below 150 s, the corresponding water depth was below 25 mm, which proved insufficient to completely suppress the smoldering peat. When the spray depth reached 25 mm, three distinct outcomes were observed: failed suppression, partial suppression, and complete suppression.

In cases of failed suppression, the smoldering peat fire evolves through four distinct stages: initial development, apparent quenching, smoldering resurgence, and burnout. The evolution of the mass fluxes of major gas species (CO_2, CO, CH_4, and NH_3) exhibits overall consistency with the transient mass loss rate of the sample. During the apparent quenching stage, all measured gas fluxes drop to near zero and fluctuate markedly, creating a misleading impression of extinguishment. However, both the time to resurgence and the time to the post-resurgence emission peak increase with greater water volume, which can guide long-term monitoring and re-inspection strategies. The peak mass fluxes and average EF values for CO_2, CO, and CH_4, as well as combustion regime indicators like MCE and CO/CO_2 ratio, show little correlation with water volume. In contrast, the peak mass flux and averaged EF of CH_4, along with the CH_4/CO_2 ratio, decrease with increasing water volume, mainly attributed to the narrowing of the pyrolysis front. Specifically, at the threshold water depth of 25 mm, the peak mass flux and EF of CH_4, as well as the CH_4/CO_2 ratio, decrease by approximately 50%.

This study provides new insights into gaseous emissions from water-suppressed smoldering peat fires. The transient mass fluxes and EFs obtained here provide important updates for current fire emission factor inventories (e.g., GFED), thereby improving carbon budget and fire emission estimates in atmospheric models. Furthermore, they provide essential data for assessing the potential health risks faced by firefighters tasked with suppressing smoldering peat fires.

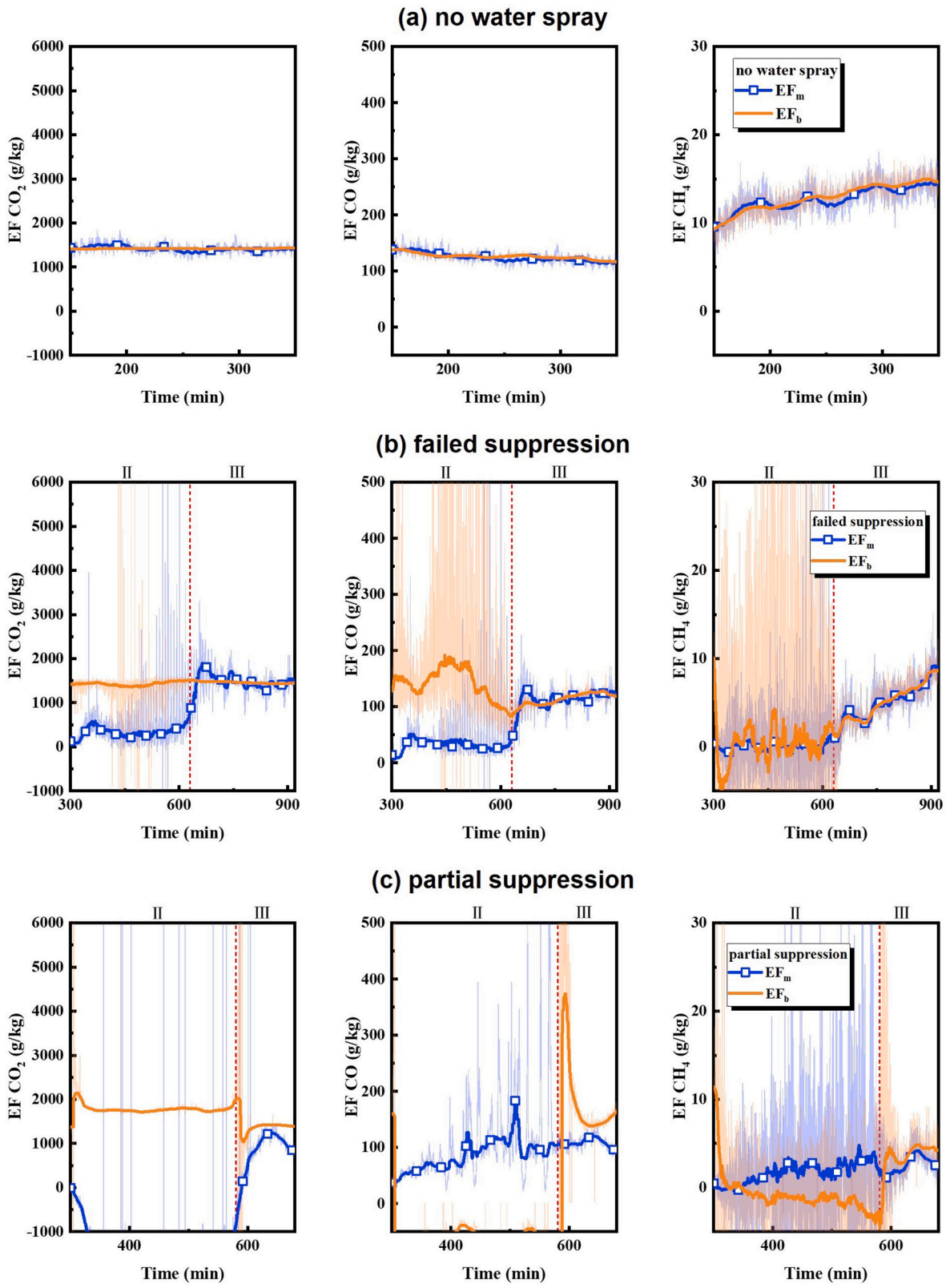

Fig. 8. Evolution of EF_m and EF_b under conditions of (a) no-water-spray, (b) failed suppression for Δt_s = 2.5 min, (c) partial suppression for Δt_s = 2.5 min.

CRediT authorship contribution statement

Yuting Jiang: Writing – original draft, Methodology, Investigation, Formal analysis, Data curation, Conceptualization. **Haoyang Qin:** Methodology. **Chuan Wan:** Data curation. **Yichao Zhang:** Writing – review & editing. **Shaorun Lin:** Writing – review & editing. **Jiuling Yang:** Writing – review & editing. **Yuqi Hu:** Writing – review & editing, Supervision, Methodology, Investigation. **Xinyan Huang:** Writing – review & editing, Supervision, Methodology.

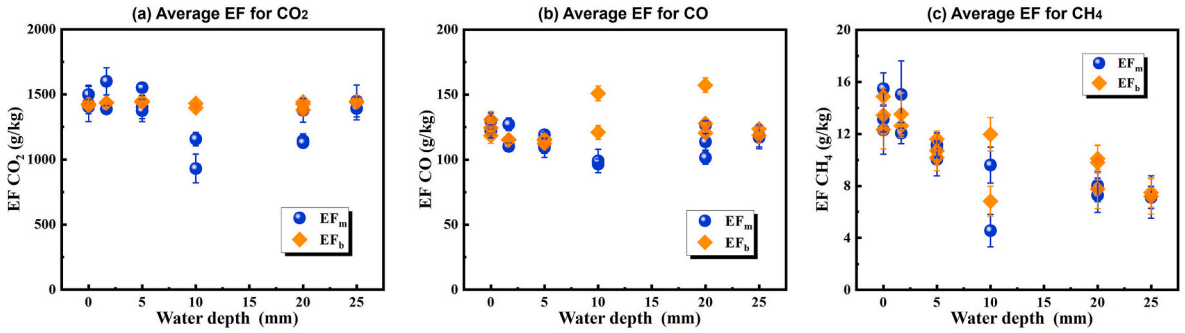

Fig. 9. Average EF_m and EF_b during the renewed steady state for CO_2, CO, and CH_4 in cases of failed suppression.

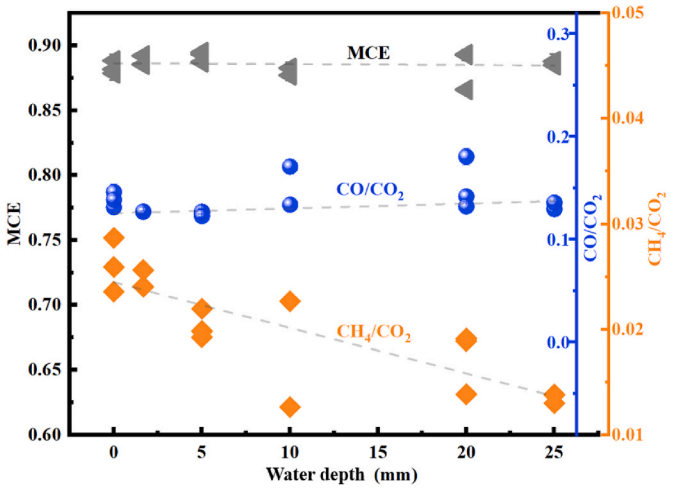

Fig. 10. Average MCE, CO/CO_2, and CH_4/CO_2 during the renewed steady state in the cases of failed suppression.

Declaration of competing interest

The authors declare that they have no known competing financial interests or personal relationships that could have appeared to influence the work reported in this paper.

Acknowledgements

This work is funded by the National Natural Science Foundation of China (No. 52106184, 52306158, and 52322610), Natural Science Foundation of Sichuan Province (2023NSFSC0189 and 2025ZNSFSC1200), Sichuan Fire Research Institution Basic Research Funds (No. Z20238801 and 20248811Z), and RGC Hong Kong GRF Scheme (No. 15221523).

Appendix A. Supplementary data

Supplementary data to this article can be found online at https://doi.org/10.1016/j.firesaf.2026.104794.

References

[1] J.T. Abatzoglou, A.P. Williams, R. Barbero, Global Emergence of Anthropogenic Climate Change in Fire Weather Indices, Geophys. Res. Lett. 46 (2018) 326–336, https://doi.org/10.1029/2018GL080959.
[2] G. Rein, Smouldering fires and natural fuels, in: Claire M. Belcher (Ed.), Fire Phenom. Earth Syst., John Wiley & Sons, Ltd., New York, 2013, pp. 15–34, https://doi.org/10.1002/9781118529539.ch2.
[3] M.A. Santoso, E.G. Christensen, J. Yang, G. Rein, Review of the transition from smouldering to flaming combustion in wildfires, Front. Mech. Eng. 5 (2019), https://doi.org/10.3389/fmech.2019.00049.
[4] T.J. Ohlemiller, Modeling of smoldering combustion propagation, Prog. Energy Combust. Sci. 11 (1985) 277–310, https://doi.org/10.1016/0360-1285(85)90004-8.
[5] J.A.S. Lighty, J.M. Veranth, A.F. Sarofim, Combustion aerosols: factors governing their size and composition and implications to human health, J. Air Waste Manag. Assoc. 50 (2000) 1565–1618, https://doi.org/10.1080/10473289.2000.10464197.
[6] Y. Hu, N. Fernandez-Anez, T.E.L. Smith, G. Rein, Review of emissions from smouldering peat fires and their contribution to regional haze episodes, Int. J. Wildland Fire 27 (2018) 293–312, https://doi.org/10.1071/WF17084.
[7] G. Rein, S. Cohen, A. Simeoni, Carbon emissions from smouldering peat in shallow and strong fronts, Proc. Combust. Inst. 32 (2009) 2489–2496, https://doi.org/10.1016/j.proci.2008.07.008.
[8] A. Usup, Y. Hashimoto, H. Takahashi, H. Hayasaka, Combustion and thermal characteristicsof peat fire in tropical peatland in Central Kalimantan, Tropics 14 (2004) 1–19, https://doi.org/10.3759/tropics.14.1.
[9] Y. Hu, E. Christensen, F. Restuccia, G. Rein, Transient gas and particle emissions from smouldering combustion of peat, Proc. Combust. Inst. 37 (2019) 4035–4042, https://doi.org/10.1016/j.proci.2018.06.008.
[10] J. Yang, H. Chen, W. Zhao, J. Zhou, Combustion kinetics and emission characteristics of peat by using TG-FTIR technique, J. Therm. Anal. Calorim. 124 (2016) 519–528, https://doi.org/10.1007/s10973-015-5168-x.
[11] L.R. Perdana, N.G. Ratnasari, M.L. Ramadhan, P. Palamba, Nasruddin, Y. S. Nugroho, Hydrophilic and hydrophobic characteristics of dry peat, IOP Conf. Ser. Earth Environ. Sci. 105 (2018), https://doi.org/10.1088/1755-1315/105/1/012083.
[12] P. Garg, S. Wang, J.M. Oakes, C. Bellini, M.J. Gollner, Variations in gaseous and particulate emissions from flaming and smoldering combustion of Douglas fir and lodgepole pine under different fuel moisture conditions, Combust. Flame 263 (2024) 113386, https://doi.org/10.1016/j.combustflame.2024.113386.
[13] Y. Hu, T.E.L. Smith, M.A. Santoso, H.M.F. Amin, E. Christensen, W. Cui, D.M. J. Purnomo, Y.S. Nugroho, G. Rein, GAMBUT field measurement of emissions from a tropical peatland fire experiment: from ignition to spread to suppression, Int. J. Wildland Fire 33 (2024) 1–22, https://doi.org/10.1071/WF23079.
[14] J. Yang, H. Wang, R. Wang, Z. Fu, Y. Hu, Experimental study of smouldering combustion and transient emissions from forest duff with dual layers, Proc. Combust. Inst. 40 (2024) 105354, https://doi.org/10.1016/j.proci.2024.105354.
[15] Y. Chen, S. Lin, Z. Liang, N.C. Surawski, X. Huang, Smouldering organic waste removal technology with smoke emissions cleaned by self-sustained flame, J. Clean. Prod. 362 (2022) 1–19, https://doi.org/10.1016/j.jclepro.2022.132363.
[16] Y. Chen, A.L. Sullivan, Z. Wang, L. Volkova, C.J. Weston, S. Lin, Y. Qin, X. Huang, N.C. Surawski, Machine learning prediction of fine woody fuel consumption in surface fires burning in eucalypt forest fuels, Int. J. Wildland Fire (2022) 1–18, https://doi.org/10.1071/WF25255.
[17] P.J. Deane, S.L. Wilkinson, G.J. Verkaik, P.A. Moore, D. Schroeder, J. M. Waddington, Peat surface compression reduces smouldering fire potential as a novel fuel treatment for boreal peatlands, Can. J. For. Res. 52 (2022) 396–405, https://doi.org/10.1139/cjfr-2021-0183.
[18] S. Wang, B.L. Bathras, W. Cui, P. Garg, S. Lin, M.J. Gollner, Flaming vs. smoldering emissions of pine needles under limited oxygen and fuel moisture conditions, Proc. Combust. Inst. 40 (2024) 105616, https://doi.org/10.1016/j.proci.2024.105616.
[19] S. Lin, Y.K. Cheung, Y. Xiao, X. Huang, Can rain suppress smoldering peat fire? Sci. Total Environ. 727 (2020) 138468 https://doi.org/10.1016/j.scitotenv.2020.138468.
[20] S.S. Vasconcelos, P.M. Fearnside, P.M.L.A. Graça, D.V. Dias, F.W.S. Correia, Variability of vegetation fires with rain and deforestation in Brazil's state of Amazonas, Remote Sens. Environ. 136 (2013) 199–209, https://doi.org/10.1016/j.rse.2013.05.005.
[21] X. Huang, G. Rein, Upward-and-downward spread of smoldering peat fire, Proc. Combust. Inst. 37 (2019) 4025–4033, https://doi.org/10.1016/j.proci.2018.05.125.
[22] S. Lin, X. Huang, An experimental method to investigate the water-based suppression of smoldering peat fire, MethodsX 7 (2020) 100934, https://doi.org/10.1016/j.mex.2020.100934.
[23] R. Hadden, G. Rein, Burning and Water Suppression of Smoldering Coal Fires in Small-Scale Laboratory Experiments, Coal and Peat Fires: A Global Perspective, Vol. 1, Elsevier B.V., 2010, 317-326, https://doi.org/10.1016/B978-0-444-52858-2.00018-9.

[24] M.A. Santoso, Experimental study of smouldering wildfire mitigation: spread, suppression and transition to flaming, 2020.
[25] M.L. Ramadhan, P. Palamba, F.A. Imran, E.A. Kosasih, Y.S. Nugroho, Experimental study of the effect of water spray on the spread of smoldering in Indonesian peat fires, Fire Saf. J. 91 (2017) 671–679, https://doi.org/10.1016/j.firesaf.2017.04.012.
[26] M.A. Santoso, W. Cui, H.M.F. Amin, E.G. Christensen, Y.S. Nugroho, G. Rein, Laboratory study on the suppression of smouldering peat wildfires: effects of flow rate and wetting agent, Int. J. Wildland Fire 30 (2021) 378–390, https://doi.org/10.1071/WF20117.
[27] R.F. Mikalsen, B.C. Hagen, A. Steen-Hansen, U. Krause, V. Frette, Extinguishing smoldering fires in wood pellets with water cooling: an experimental study, Fire Technol. 55 (2018) 257–284, https://doi.org/10.1007/s10694-018-0789-9.
[28] Y. Qin, Y. Zhang, Y. Chen, S. Lin, Y. Shu, Y. Huang, X. Huang, M. Zhou, Impact of snow on underground smoldering wildfire in arctic-boreal peatlands, Environ. Sci. Technol. 59 (2025) 3915–3924, https://doi.org/10.1021/acs.est.4c08569.
[29] A. Witze, Why arctic fires are bad news for climate change, Nature 585 (2020) 336–337.
[30] Y. Zhang, Y. Chen, Y. Qin, Y. Li, Y. Zhou, Z. Zhang, Y. Jiang, S. Lin, X. Huang, Suppressing underground peat fire and smoldering spread via water, ice, dry ice, and liquid nitrogen, Fire Saf. J. 162 (2026) 104772, https://doi.org/10.1016/j.firesaf.2026.104772.
[31] S. Lin, Y. Liu, X. Huang, How to build a firebreak to stop smouldering peat fire: insights from a laboratory-scale study, Int. J. Wildland Fire 30 (2021) 454–461, https://doi.org/10.1071/WF20155.
[32] G.R. Van Der We, T.R. James, D. Van Wees, Y. Chen, L. Gi, J. Ha, R. Vernooij, M. Mingquan, B. Samiha, Landscape fire emissions from the 5 th version of the global fire emissions database (GFED5), Sci. Data 12 (2025) 1870, https://doi.org/10.1038/s41597-025-06127-w.
[33] X. Huang, F. Restuccia, M. Gramola, G. Rein, Experimental study of the formation and collapse of an overhang in the lateral spread of smouldering peat fires, Combust. Flame 168 (2016) 393–402, https://doi.org/10.1016/j.combustflame.2016.01.017.
[34] J. Yang, N. Liu, H. Chen, W. Gao, R. Tu, Effects of atmospheric oxygen on horizontal peat smoldering fires: experimental and numerical study, Proc. Combust. Inst. (2018) 1–9, https://doi.org/10.1016/j.proci.2018.06.218, 000.
[35] Y. Qin, Y. Chen, Y. Zhang, S. Lin, X. Huang, Modeling smothering limit of smoldering combustion: oxygen supply, fuel density, and moisture content, Combust. Flame 269 (2024) 113683, https://doi.org/10.1016/j.combustflame.2024.113683.
[36] S. Lin, X. Huang, Quenching of smoldering: effect of wall cooling on extinction, Proc. Combust. Inst. 38 (2021) 5015–5022, https://doi.org/10.1016/j.proci.2020.05.017.
[37] S. Lin, H. Yuan, X. Huang, A computational study on the quenching and near-limit propagation of smoldering combustion, Combust. Flame 238 (2022) 111937, https://doi.org/10.1016/j.combustflame.2021.111937.
[38] D. Shaposhnikov, B. Revich, T. Bellander, G.B. Bedada, M. Bottai, T. Kharkova, E. Kvasha, E. Lezina, T. Lind, E. Semutnikova, G. Pershagen, Mortality related to air pollution with the Moscow heat wave and wildfire of 2010, Epidemiology 25 (2014) 359–364, https://doi.org/10.1097/EDE.0000000000000090.
[39] C.E. Stockwell, T. Jayarathne, M.A. Cochrane, K.C. Ryan, E.I. Putra, B.H. Saharjo, A.D. Nurhayati, I. Albar, D.R. Blake, I.J. Simpson, E.A. Stone, R.J. Yokelson, Field measurements of trace gases and aerosols emitted by peat fires in Central Kalimantan, Indonesia, during the 2015 El Niño, Atmos. Chem. Phys. 16 (2016) 11711–11732, https://doi.org/10.5194/acp-16-11711-2016.
[40] C. Paton-Walsh, T.E.L. Smith, E.L. Young, D.W.T. Griffith, A. Guérette, New emission factors for Australian vegetation fires measured using open-path Fourier transform infrared spectroscopy - part 1: methods and Australian temperate forest fires, Atmos. Chem. Phys. 14 (2014) 11313–11333, https://doi.org/10.5194/acp-14-11313-2014.
[41] D. Wilson, S.D. Dixon, R.R.E. Artz, T.E.L. Smith, C.D. Evans, H.J.F. Owen, E. Archer, F. Renou-Wilson, Derivation of greenhouse gas emission factors for peatlands managed for extraction in the Republic of Ireland and the United Kingdom, Biogeosciences 12 (2015) 5291–5308, https://doi.org/10.5194/bg-12-5291-2015.
[42] Y. Chen, S. Lin, Y. Qin, N.C. Surawski, X. Huang, Carbon distribution and multi-criteria decision analysis of flexible waste biomass smouldering processing technologies, Waste Manag. 167 (2023) 183–193, https://doi.org/10.1016/j.wasman.2023.05.038.
[43] T.R. Muraleedharan, M. Radojevic, A. Waugh, A. Caruana, Emissions from the combustion of peat: an experimental study, Atmos. Environ. 34 (2000) 3033–3035, https://doi.org/10.1016/S1352-2310(99)00512-9.
[44] T.J. Christian, B. Kleiss, R.J. Yokelson, R. Holzinger, P.J. Crutzen, W.M. Hao, B. H. Saharjo, D.E. Ward, Comprehensive laboratory measurements of biomass-burning emissions: 1. Emissions from Indonesian, African, and other fuels, J. Geophys. Res. Atmos. 108 (2003) 4719, https://doi.org/10.1029/2003jd003704.